Carbohydrate Polymers 121 (2015) 49–55

Contents lists available at ScienceDirect

Carbohydrate Polymers

journal homepage: www.elsevier.com/locate/carbpol

Fluorescent nanoparticles from starch: Facile preparation, tunable luminescence and bioimaging

Meiying Liu[a], Xiqi Zhang[b], Bin Yang[b], Zhan Li[c], Fengjie Deng[a], Yang Yang[a], Xiaoyong Zhang[a,b,*], Yen Wei[b,**]

[a] Department of Chemistry/Institute of Polymers, Nanchang University, 999 Xuefu Avenue, Nanchang 330031, China
[b] Department of Chemistry and the Tsinghua Center for Frontier Polymer Research, Tsinghua University, Beijing 100084, China
[c] Key Laboratory of Chemistry of Northwestern Plant Resources, Key Laboratory for Natural Medicine of Gansu Province, Institute of Chemical Physics, Chinese Academy of Sciences, Lanzhou, Gansu 730000, China

ARTICLE INFO

Article history:
Received 14 November 2014
Received in revised form 2 December 2014
Accepted 4 December 2014
Available online 3 January 2015

Keywords:
Starch
Polyethyleneimine
Fluorescent organic nanoparticles
Cell imaging
Biomedical applications

ABSTRACT

Fluorescent organic nanoparticles (FONs) based on carbohydrate polymers were prepared through one-pot hydrothermal treatment of starch in the presence of polyethyleneimine. These FONs (named as *PEI-Starch* FONs) were characterized by a series of techniques including UV–Vis absorption spectroscopy, fluorescent spectroscopy, Fourier transform infrared spectroscopy, transmission electron microscopy and X-ray photoelectron spectroscopy. Results showed that the size of PEI-Starch FONs is 10–30 nm. The PEI-Starch FONs exhibited high water dispersibility because of the existence of hydrophilic functional groups on their surface. After excited with different wavelength, PEI-Starch FONs emitted strong and excitation-dependent fluorescence. To evaluate their potential for biomedical applications, biocompatibility and cell uptake behavior of PEI-Starch FONs were further investigated. We demonstrated that PEI-Starch FONs are biocompatible with cells and can be easily internalized by cells within 3 h. Taken together, novel FONs have been prepared via a simple and scalable hydrothermal method using starch and polyethyleneimine as precursors. These PEI-Starch FONs showed excellent fluorescence properties, high water dispersibility and good biocompatibility, making them highly potential for various biomedical applications.

1. Introduction

With the rapid development of nanoscience and nanotechnology, searching of novel fluorescent nanomaterials for biomedical applications has attracted increasing research interest (Bhirde, Xie, Swierczewska, & Chen, 2011; Kim, Piao, & Hyeon, 2009; Rosi & Mirkin, 2005; Weissleder, 2006). Great effort has been devoted toward these areas and a number of bioprobes based on nanomaterials, which composed with inorganic and organic components have been developed (Ding, Li, Liu, & Tang, 2013; Michalet et al., 2005; Zhang, Zhang, tao, et al., 2014; Zhang, Zhang, Yang, Zhang, & Wei, 2014). As compared with small organic dyes, fluorescent nanomaterials are normally exhibited better optical properties and can be easily integrated with other functional components including targeting agents and drugs, etc. (Boisselier & Astruc, 2009; Breul, Hager, & Schubert, 2013; Feng et al., 2013). Since the first report of using semiconduct quantum dots for bioimaging applications (Bruchez, Moronne, Gin, Weiss, & Alivisatos, 1998; Chan & Nie, 1998), many fluorescent inorganic nanoparticles (FINs) including silicon quantum dots, lanthanide ions doped nanomaterials, carbon quantum dots and fluorescent metal clusters have been developed for biomedical applications (Boisselier & Astruc, 2009; Chandra, Das, Bag, Laha, & Pramanik, 2011; Díez & Ras, 2011; Hui et al., 2012; Liu, Zhang, Qiao, & Su, 2012; Luo et al., 2014; Mitra et al., 2012; Sena & Gao, 2010; Zhang, Hui, Yang, et al., 2013; Zhang, Wang, Liu, et al., 2013; Zhang, Wang, Zhu, et al., 2013; Zhang, Zhang, Yang, et al., 2014). Although great advance has been achieved in biomedical applications of FINs, the accumulation of FINs in reticuloendothelial system (RES), non-biodegradability and potential toxicity have significantly limited their practical biomedical applications (Choi et al., 2007; Gao, Cui, Levenson, Chung, & Nie, 2004). It is therefore development of novel fluorescent nanoprobes which could overcome these obvious disadvantages of FINs should be of great importance.

* Corresponding author at: Department of Chemistry/Institute of Polymers, Nanchang University, 999 Xuefu Avenue, Nanchang 330031, China.
Tel.: +86 01062792604.
** Corresponding author.
E-mail addresses: xiaoyongzhang1980@gmail.com (X. Zhang), weiyen@tsinghua.edu.cn (Y. Wei).

http://dx.doi.org/10.1016/j.carbpol.2014.12.047
0144-8617/

As compared with FINs, fluorescent organic nanoparticles (FONs) have recently received increasing attention for biomedical applications because of their flexible synthesis strategies, designability of small organic molecules, ease of surface functionalization, biodegradable potential and good biocompatibility (Feng et al., 2013; Li & Liu, 2014; Qin, Lam, & Tang, 2012). To date, a series of FONs based on small organic dyes, conjugated polymers, aggregation induced emission (AIE) dyes or aggregation induced enhancement of emission (AIEE) dyes have been emerging as fluorescent probes for biomedical applications (Ding et al., 2013; Kim, Ohulchanskyy, Pudavar, Pandey, & Prasad, 2007; Liu, Zhang, Yang, Deng, et al., 2014; Liu, Zhang, Yang, Liu, et al., 2014; Thomas, Joly, & Swager, 2007; Wang, Yuan, et al., 2014; Yu et al., 2013; Zhang, Zhang, Yang, et al., 2014; Zhang, Zhang, Yang, Zhang, et al., 2014; Zhao et al., 2008, 2010). Different strategies including encapsulation of hydrophobic dyes using commercial and synthetic amphiphilic polymers, covalently conjugation of dyes with hydrophobic molecules via Schiff-base or ring-opening reaction, and incorporation of polymerizable dyes with other monomers through polymerization reaction have been utilized to fabricate various FONs (Qin et al., 2012b; Zhang, Zhang, Yang, et al., 2013; Zhang, Zhang, Yang, Hui, et al., 2014; Zhang, Zhang, Yang, Liu, et al., 2014; Zhang, Zhang, Yang, Liu, Liu, et al., 2014). The basic principle for fabrication of FONs is to prepare dye contained amphiphilic polymers, which can be further self-assembled into fluorescent core–shell nanoparticles in aqueous solution (Breul et al., 2013). However, there still have a number of problems for fabrication of FONs for biomedical applications. For example, fluorescence intensity of FONs based on conventional organic dyes will be significantly decreased because of the notorious aggregation caused quenching (ACQ) effect (Leung et al., 2013). Dyes with AIE or AIEE properties could overcome the ACQ effect of conventional organic dyes, however, the synthesis of small organic dyes is rather complex and tedious. On the other hand, high cost small organic precursors and hazardous organic solvents are generally required to synthesis these dyes. Therefore, the development of a simple method for preparation of novel FONs, which showed excellent fluorescent properties, high water dispersibility and good biocompatibility using low cost precursors is highly desirable.

Starch is a type of natural, renewable and biodegradable polymers. Due to its biocompatibility, non-immunogenicity, stability in the air, abundant and low cost, starch has been an attractive substitute for preparation of starch based nanoparticles for various applications (Ma, Jian, Chang, & Yu, 2008; Moreira, Pedro, Glenn, Marconcini, & Mattoso, 2013; Shi, Wang, Li, & Adhikari, 2013; Tay, Pang, & Chin, 2012; Xie, Pollet, Halley, & Averous, 2013). A numerous of previous reports have demonstrated that starch based nanoparticles could be prepared through cold acid hydrolysis, high power ultrasonication, high-pressure homogenization, gamma irradiation and miniemulsion cross-linking, and nanoprecipitation (Bel Haaj, Magnin, Pétrier, & Boufi, 2013; Chin, Pang, & Tay, 2011; Kim, Han, Kweon, Park, & Lim, 2013; Lamanna, Morales, García, & Goyanes, 2013; Shi, Li, Wang, Li, & Adhikari, 2011). Recently, the preparation of luminescent starch nanoparticles has also demonstrated via self-assembly of fluorescein-labeled starch acetate in water (Li et al., 2011). The utilization of fluorescein-labeled starch maleate nanoparticles for metal ions sensing has also been reported by Chin, Azman, Pang, and Ng (2014). However, to the best of our knowledge, limited effort has been focused on the preparation of fluorescent starch based nanoparticles without linkage starch with small organic dyes. In the present study, we reported a method for preparation of starch based FONs via one-step hydrothermal treatment of starch in the presence of polyethyleneimine (PEI). This method is rather simple, cost effective and scalable. Thus obtained FONs (named as PEI-Starch FONs) were characterized by a series of characterization techniques including UV–Vis absorption spectroscopy, fluorescent spectroscopy, Fourier transform infrared spectroscopy (FT-IR), transmission electron microscopy (TEM), X-ray photoelectron spectroscopy (XPS). To explore their biomedical applications, biocompatibility as well as cell uptake behavior of PEI-Starch FONs were further evaluated.

2. Experimental

2.1. Materials and measurements

Polyethyleneimine (PEI, Mw = 600, Alading Reagent Inc.), water soluble starch (Alading Reagent Inc.) were used as received. All the other solvents and chemicals were purchased from commercial sources and used directly without further purification.

UV–Vis absorption spectra were recorded on UV/Vis/NIR Perkin-Elmer lambda750 spectrometer (Waltham, MA, USA) using quartz cuvettes of 1 cm path length. Fluorescence spectra were measured on a PE LS-55 spectrometer with a slit width of 3 nm for both excitation and emission to obtain suitable fluorescent intensity. The FT-IR spectra were obtained in a transmission mode on a Perkin-Elmer Spectrum 100 spectrometer (Waltham, MA, USA). Typically, 8 scans at a resolution of 1 cm^{-1} were accumulated to obtain one spectrum. The XPS spectra were performed on a VGESCALAB 220-IXL spectrometer using an Al Kα X-ray source (1486.6 eV). The energy scale was internally calibrated by referencing to the binding energy (E_b) of the C1s peak of a carbon contaminant at 284.6 eV. Transmission electron microscopy (TEM) images were recorded on a JEM-1200EX microscope operated at 100 kV, the TEM specimens were made by placing a drop of the nanoparticles suspension on a carbon-coated copper grid. The size distribution of PEI-Starch FONs in water was determined using a zeta Plus apparatus (ZetaPlus, Brookhaven Instruments, Holtsville, NY).

Fluorescence quantum yield was measured according to established procedure in our previous reports (Zhang, Wang, Liu, et al., 2013). The optical densities were measured on UV–Vis spectra were obtained on a UV/Vis/NIR Perkin-Elmer lambda750 Spectrophotometer. Quinine sulfate in 0.1 M H_2SO_4 (literature quantum yield 0.54 at 360 nm) was chose as a standard (Shen, Yao & Lu, 2013). Absolute values are calculated using the standard reference sample that has a fixed and known fluorescence quantum yield value, according to the following equation:

$$\varphi_X = \varphi_{std} \frac{I_x}{A_x} \frac{A_{std}}{I_{std}} \left| \frac{\eta_x^2}{\eta_{std}^2} \right|$$

where φ is the quantum yield, I is the measured integrated emission intensity, and A is the optical density, and η is the refractive index. The subscript "*std*" refers to the reference fluorophore of known quantum yield. In order to minimize re-absorption effects absorbencies in the 10 mm fluorescence cuvette were kept under 0.1 at the excitation wavelength (360 nm).

2.2. Preparation of PEI-Starch FONs

PEI-Starch FONs were prepared by hydrothermal treatment of starch and PEI. Briefly, starch (300 mg) and PEI (150 mg) were dissolved in 20 mL deionized water with magnetic stirring. And then the mixture was heated to 100 °C for 2 h. Thus obtained FONs were purified by dialysis through porous cellulose dialysis bag (molecular weight cut off 7000 Da) using ethanol to remove the unreacted PEI. Finally the product inside the dialysis bag was collected and dried by vacuum oven at 40 °C.

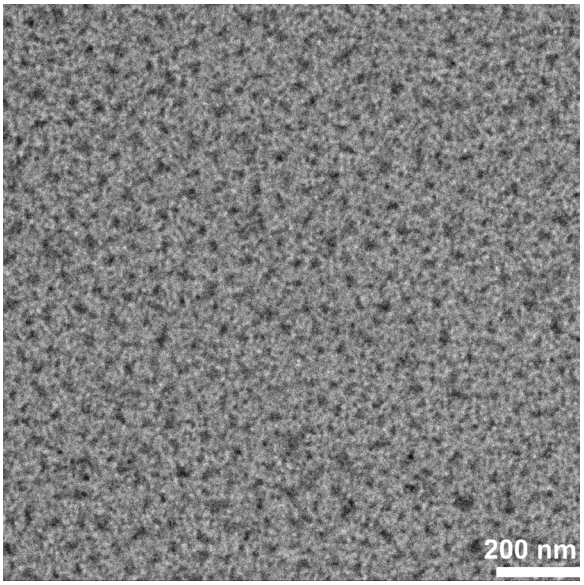

Fig. 1. Representation TEM image of PEI-Starch FONs, scale bar = 200 nm. A lot of nanoparticles with diameter at 10–30 nm can be identified from the TEM image.

2.3. Cytotoxicity of PEI-Starch FONs

Cell morphology was examined to evaluate the effects of PEI-Starch FONs to HepG2 cells. Cells were treated with complete cell culture medium, or different concentrations of PEI-Starch FONs prepared in 10% FBS containing media for 24 h. The morphology of cells was observed by using an optical microscopy (Leica, Germany), the overall magnification was 100×.

The cell viability of PEI-Starch FONs on HepG2 cells was evaluated by cell counting kit-8 (CCK-8) assay based on our previous report (Zhang, Qi, et al., 2012). Cells were incubated with 10, 20, 40, 80, 120 μg mL^{-1} PEI-Starch FONs for 8 and 24 h. Plates were then analyzed with a microplate reader (Victor XIII, Perkin-Elmer) at 450 nm with the reference wavelength at 620 nm. Cell survival was expressed as absorbance relative to that of untreated controls. Results are presented as mean ± standard deviation (SD).

2.4. Confocal microscopic imaging of cells using PEI-Starch FONs

To evaluate the bioimaging potential of PEI-Starch FONs. Cells were incubated with 20 μg mL^{-1} of PEI-Starch FONs for 3 h at 37 °C (Yang et al., 2012). Afterward, the cells were washed three times with PBS to remove the PEI-Starch FONs and then fixed with 4% paraformaldehyde for 10 min at room temperature. Cell images were taken with a confocal laser scanning microscope (CLSM) Zesis 710 3-channel (Zesis, Germany) with the excitation wavelength of 405 and 458 nm.

3. Results and discussion

3.1. Characterization of PEI-Starch FONs

Fig. 1 shows the TEM image of PEI-Starch FONs. Many irregular particles with size at 10–30 nm can be found in the sample of PEI-Starch FONs. These results given the direct evidence that we have successfully prepared starch based nanoparticles. We have tried to obtain high resolution TEM images, however, the images of nanoparticles became rather blur possible due to their low contrast. The hydrodynamic size distribution of PEI-Starch FONs in water was also determined by dynamic laser scattering (DLS). The results showed that size of PEI-Starch FONs by DLS is 194.9 ± 35.5 nm with a polydispersity index of 0.225 (Fig. 2).

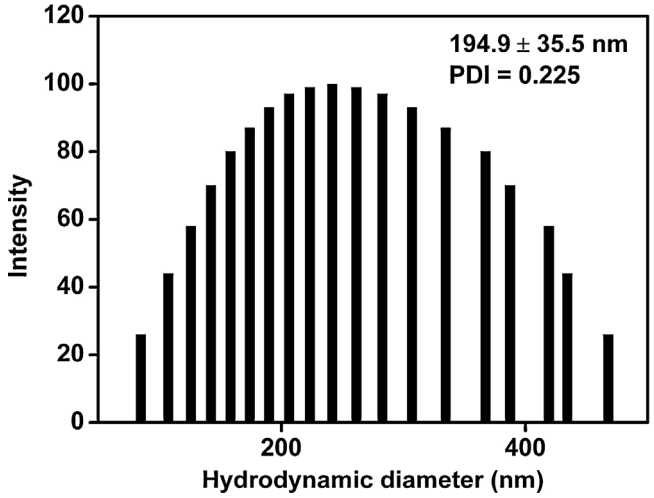

Fig. 2. Hydrodynamic size of PEI-Starch FONs in water determined by DLS.

The PEI-Starch FONs was further evaluated by FT-IR. As shown in Fig. S1, a strong absorption peak at around 3380 cm^{-1} was observed in the samples of starch and PEI-Starch FONs, suggesting that –OH group was existed in PEI-Starch FONs. On the other hand, two peaks centered at 2940 and 2820 cm^{-1} can be observed in PEI, which can be assigned to the stretching vibration of C–H bond (Cao et al., 2013). As compared with spectrum of starch, absorption intensity of PEI-Starch FONs located at 1280–1522 cm^{-1} and 1522–1707 cm^{-1} has significantly enhanced. These results suggested that functional groups such as N–H, C=O and C=C were possibly existed in the sample of PEI-Starch FONs. The FT-IR results also implied that we have successfully prepared PEI-Starch FONs. Furthermore, chemical compositions of PEI-Starch FONs were characterized by XPS. As shown in Fig. 3A, three elements (C, N and O) were detected by XPS spectra of survey scan from 0–1200 eV. This given a direct evidence that we have obtained PEI-Starch FONs. The detailed information about XPS spectra was shown in Fig. 3B and D. An intensive peak at 284.6 eV can be observed in spectrum of C1s, which can be assigned to C–C bond. On the other hand, a shoulder peak at 287.6 eV can also be found in the C1s spectrum, which indicated that C–O and C=O were existed in PEI-Starch FONs. The binding energy peak of N1s at 399.2 eV can be observed in Fig. 3C, suggesting that C–N bond was existed in the sample of PEI-Starch FONs. The O1s spectrum of PEI-Starch FONs shows a main peak at 531.2 eV, which can be ascribed to the C–O and C=O bonds. All of these XPS spectra suggested that PEI has successfully incorporated into PEI-Starch FONs. The concentration of elements such as C, N and O in the sample of PEI-Starch FONs was also calculated based on XPS spectra. The mass percentages of C, N and O in PEI-Starch FONs are 71.0, 11.85 and 17.15, respectively. As compared with the theoretical value of starch, the mass percentage of C is significantly increased from 42.1% to 71.0%, while O is decreased from 51.5% to 17.15%. Based on the mass percentage of N in PEI and PEI-Starch FONs, the mass ratio of starch and PEI is calculated to be 1.75:1, which is very closed to their feed ratio (2:1).

Due to the existence of hydrophilic functional groups such as –OH, NH_2, NH and C=O on the surface of PEI-Starch FONs, thus obtained nanoparticles exhibited high water dispersibility. No precipitation was observed when PEI-Starch FONs were deposited for more than one month (left cuvette in Fig. S2). After irradiated with UV lamp at 365 nm, strong blue fluorescence can be observed (light cuvette in Fig. S2). The detailed luminescent properties of PEI-Starch FONs were further characterized by fluorescence

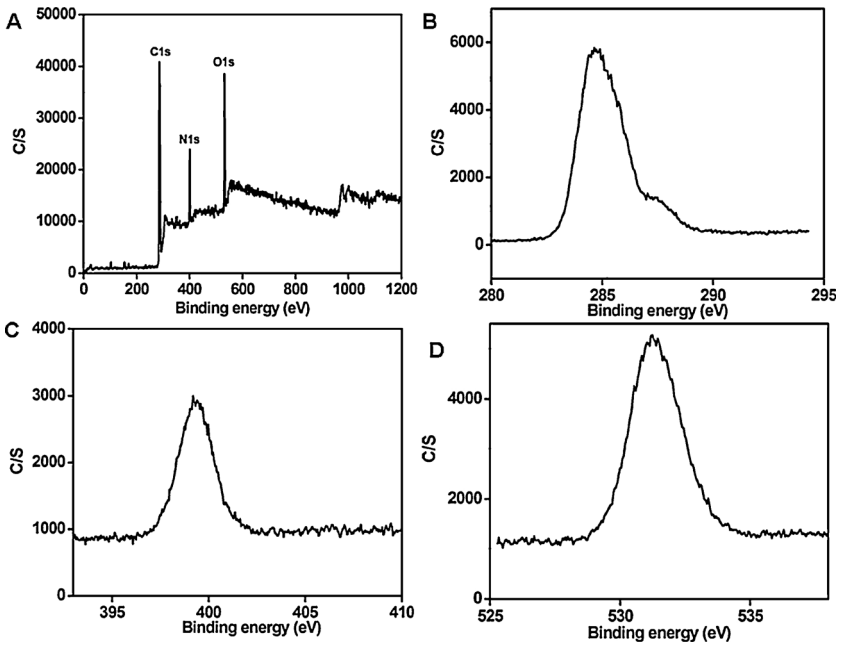

Fig. 3. XPS spectra of PEI-Starch FONs. (A) Survey scan of XPS spectra, (B) C1s region, (C) N1s region, (D) O1s region. The XPS spectra suggested that elements including C, N and O were existed in the sample of PEI-Starch FONs.

spectroscopy. As shown in Fig. 4, PEI-Starch FONs can be excited by various excitation wavelength ranged from 360 to 480 nm, and their emission peaks were also red shifted from 460 to 550 nm, correspondingly (Fig. S3). On the other hand, the fluorescence intensity also decreased when PEI-Starch FONs were excited with different wavelength from 360 to 480 nm (Fig. 4). Based on the excitation spectra of PEI-Starch FONs, a maximum excitation intensity could be achieved at around 340 nm, and then rapidly decreased from 340 to 480 nm. The excitation spectra of PEI-Starch FONs is well consistent with their emission spectra. The excitation-dependent fluorescent properties of PEI-Starch FONs have also been reported by some other types of fluorescent nanoparticles such as carbon quantum dots (Zhang, Wang, Liu, et al., 2013). The possible reason for the excitation-dependent fluorescent properties of PEI-Starch FONs is likely due to different chromophores were existed in PEI-Starch FONs. When PEI-Starch FONs were excited by different wavelength, the emission efficiency of these chromophores may also be significant different (Wei et al., 2007).

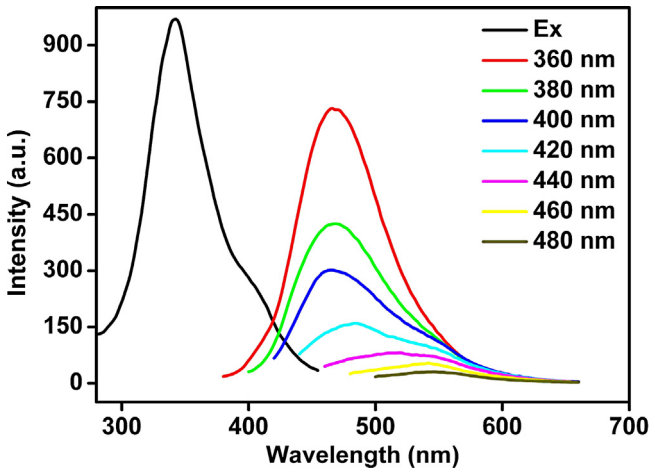

Fig. 4. PL spectra of PEI-Starch FONs (in water). The excitation peak is located at 341 nm when the emission peak was set at 480 nm. When PEI-Starch FONs were excited with different wavelength ranged from 360 to 480 nm, their emission peaks were red shift from 470 to 550 nm, correspondingly.

The possible mechanism for generation of fluorescence from PEI-Starch FONs was discussed based on our characterization results and previous reports (De & Karak, 2013; Falco, Baccile, & Titirici, 2011; Titirici, Antonietti, & Baccile, 2008). As indicated by the FT-IR and XPS results, many functional groups such as C=C and C=N bonds may formed after hydrothermal treatment of starch in the presence of PEI. On the other hand, previous reports have also demonstrated that carbohydrate polymers could hydrolysed under alkaline or acid environment. During hydrolysis, many reactive groups such as aldehyde, carbonyl groups, furan rings and ethers are generated under hydrothermal treatment (De & Karak, 2013; Falco et al., 2011; Titirici et al., 2008). These starch derivatives with functional groups could further react with PEI. We speculated that the formation of PEI-Starch FONs is likely due to copolymerization of starch and PEI under hydrothermal treatment. It has been reported that glutaraldehyde with C=C double bonds could react with the amino group of chitosan through formation of Schiff's bases. After crosslinking the free amino group by aldehyde groups, new unsaturated double bonds (C=N bonds) from the Schiff's base were generated. They speculated that the emission of crosslinked chitosan microsphere might be attributed to the $n-\pi^*$ transitions of C=N bonds in Schiff's base and the $\pi-\pi^*$ transition of C=C double bonds (Wei et al., 2007, 2008). More recently, the red emissive cross-linked chitosan nanoparticles with long wavelengths were also prepared by Wang et al. They demonstrated that apart from the mechanism proposed by Wei et al., the rearrangements of the C=N and C=C bonds, resulting in formation of pyridinium and hexahydropyridine ring structures on chitosan may also take place during cross-linkage of chitosan with glutaraldehyde (Wang, Yuan, Guo, Xu, & Chen, 2014). However, due to the finally chemical structure and reaction procedure is rather complex, the detailed mechanism for formation of the autofluorescence by PEI-Starch FONs still cannot be well defined.

Fluorescence quantum yield is an important photophysical property of fluorescent materials. In this work, the quantum yield of PEI-Starch FONs was measured according to established procedure using quinine sulfate as reference (Zhang, Zhang, Yang,

Liu, & Wei, 2014). We demonstrated that quantum yield of PEI-Starch FONs is as high as 9.8%. Given their suitable size, excellent fluorescent properties and excellent water dispersibility, PEI-Starch FONs are expected highly potential for bioimaging applications.

3.2. Biocompatibility evaluation of PEI-Starch FONs

Biocompatibility is very important for biomedical applications of biomaterials. Herein, the biocompatibility of PEI-Starch FONs to HepG2 cells was determined using optical microscopy observation and cell viability determination (Li et al., 2010). As shown in Fig. S4, cells still adhered to cell plate very well even the concentration of PEI-Starch FONs is as high as 120 μg mL^{-1}. And no significant cell morphology change was observed when cells were incubated with 120 μg mL^{-1} of PEI-Starch FONs for 24 h (Fig. S4D). These results implied that PEI-Starch FONs are biocompatible with HepG2 cells. Furthermore, the cell viability of PEI-Starch FONs were quantitatively evaluated using CCK-8 assay. HepG2 cells were incubated with different concentrations of PEI-Starch FONs for 8 and 24 h (Qi et al., 2013; Zhang et al., 2013b). As shown in Fig. 5, no cell viability decrease was observed when cells were incubated with 10–120 μg mL^{-1} of PEI-Starch FONs for 8 h. Even the incubation time was up to 24 h, cell viability of PEI-Starch FONs was still greater than 90% at concentration of 120 μg mL^{-1}, further confirming the excellent biocompatibility of PEI-Starch FONs.

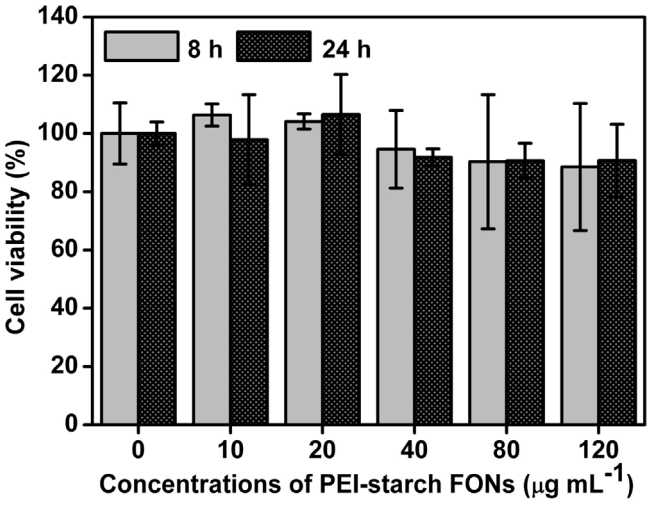

Fig. 5. Biocompatibility evaluation of PEI-Starch FONs. HepG2 cells were incubated with PEI-Starch FONs for 8 and 24 h. The concentrations of PEI-Starch FONs are ranged from 10 to 120 μg mL^{-1}. Cell viability of PEI-Starch FONs was determined by CCK-8 assay.

3.3. CLSM images of PEI-Starch FONs

The cell uptake behavior of PEI-Starch FONs was evaluated by CLSM to examine their biomedical application potential. As shown

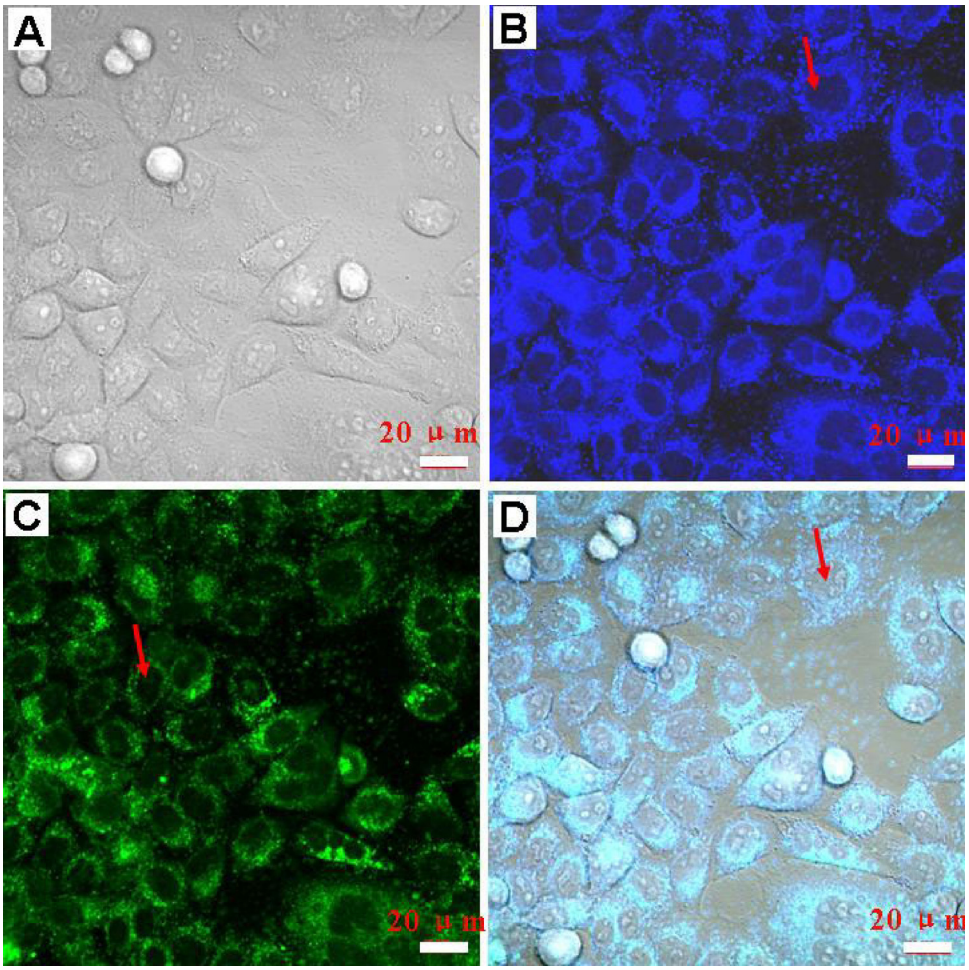

Fig. 6. CLSM images of PEI-Starch FONs. PEI-Starch FONs were incubated with HepG2 cells for 3 h. And the concentration of PEI-Starch FONs is 20 μg mL^{-1}. (A) bright field, (B) excited with 405 nm laser, (C) excited with 458 nm laser, (D) merge image of A, B and C, scale bar = 20 μm.

in Fig. 6, cell uptake of PEI-Starch FONs was clearly observed after cells were incubated with 20 μg mL^{-1} of PEI-Starch FONs for 3 h. Many dark areas with relative weak fluorescence intensity surrounded by the bright areas (fluorescence from PEI-Starch FONs) can also be observed from CLSM images (Fig. 6B). These dark areas are possible for the location of cell nucleus, indicating that PEI-Starch FONs cannot enter into cell nucleus. The successful dying of cells with PEI-Starch FONs implied that PEI-Starch FONs can potentially used for biological imaging applications. On the other hand, due to their tunable fluorescence, cell uptake of PEI-Starch FONs could be excited by lasers with different wavelength. As shown in Fig. 6B and C, cells could emit blue and green fluorescence when cells were irradiated with 405 and 458 nm wavelength laser. These results implied that PEI-Starch FONs can be used as fluorescent probes for multi-color imaging. More importantly, the dosage of PEI-Starch FONs for cell imaging is only 20 μg mL^{-1}, which is much lower than their biocompatible dosage. If PEI-Starch FONs were conjugated with targeting agents, the dosage of PEI-Starch FONs could be further decreased. Furthermore, PEI is a commercial available polymer, which has been extensively used for surface modification of nanocomposites for biomedical applications. It has been demonstrated that PEI could be used for binding negative genes or drugs due to their abundant amino groups. Therefore, multifunctional theranostics system based on PEI-Starch FONs can be facilely fabricated (Li et al., 2010; Tian et al., 2005).

4. Conclusions

In summary, we have developed a novel method for fabrication of PEI-Starch FONs through one-pot hydrothermal treatment of starch and PEI under relative low temperature (100 °C) and air atmosphere without needing catalysts and initiators. The method described in this work is rather simple, low-cost and scalable. The PEI-Starch FONs showed high water dispersibility, strong and tunable fluorescence, high fluorescence quantum yield and excellent biocompatibility, making them highly potential for different biomedical applications.

Acknowledgements

This research was supported by the National Natural Science Foundation of China (Nos. 21134004, 21201108, 51363016), and the National 973 Project (No. 2011CB935700).

Appendix A. Supplementary data

Supplementary material related to this article can be found, in the online version, at http://dx.doi.org/10.1016/j.carbpol.2014.12.047.

References

Bel Haaj, S., Magnin, A., Pétrier, C., & Boufi, S. (2013). Starch nanoparticles formation via high power ultrasonication. *Carbohydrate Polymers*, *92*(2), 1625–1632.
Bhirde, A., Xie, J., Swierczewska, M., & Chen, X. (2011). Nanoparticles for cell labeling. *Nanoscale*, *3*(1), 142–153.
Boisselier, E., & Astruc, D. (2009). Gold nanoparticles in nanomedicine: Preparations, imaging, diagnostics, therapies and toxicity. *Chemical Society Reviews*, *38*(6), 1759–1782.
Breul, A. M., Hager, M. D., & Schubert, U. S. (2013). Fluorescent monomers as building blocks for dye labeled polymers: Synthesis and application in energy conversion, biolabeling and sensors. *Chemical Society Reviews*, *42*(12), 5366–5407.
Bruchez, M., Moronne, M., Gin, P., Weiss, S., & Alivisatos, A. P. (1998). Semiconductor nanocrystals as fluorescent biological labels. *Science*, *281*(5385), 2013–2016.
Cao, Y., Zhang, X., Tao, L., Li, K., Xue, Z., Feng, L., et al. (2013). Mussel-inspired chemistry and Michael addition reaction for efficient oil/water separation. *ACS Applied Materials and Interfaces*, *5*(10), 4438–4442.
Chan, W. C., & Nie, S. (1998). Quantum dot bioconjugates for ultrasensitive nonisotopic detection. *Science*, *281*(5385), 2016–2018.
Chandra, S., Das, P., Bag, S., Laha, D., & Pramanik, P. (2011). Synthesis, functionalization and bioimaging applications of highly fluorescent carbon nanoparticles. *Nanoscale*, *3*(4), 1533–1540.
Chin, S. F., Azman, A., Pang, S. C., & Ng, S. M. (2014). Fluorescein-labeled starch maleate nanoparticles as sensitive fluorescent sensing probes for metal ions. *Journal of Nanomaterials*, http://dx.doi.org/10.1155/2014/108359
Chin, S. F., Pang, S. C., & Tay, S. H. (2011). Size controlled synthesis of starch nanoparticles by a simple nanoprecipitation method. *Carbohydrate Polymers*, *86*(4), 1817–1819.
Choi, H. S., Liu, W., Misra, P., Tanaka, E., Zimmer, J. P., Ipe, B. I., et al. (2007). Renal clearance of quantum dots. *Nature Biotechnology*, *25*(10), 1165–1170.
Díez, I., & Ras, R. H. A. (2011). Fluorescent silver nanoclusters. *Nanoscale*, *3*(5), 1963–1970.
De, B., & Karak, N. (2013). A green and facile approach for the synthesis of water soluble fluorescent carbon dots from banana juice. *RSC Advances*, *3*(22), 8286–8290.
Ding, D., Li, K., Liu, B., & Tang, B. Z. (2013). Bioprobes based on AIE fluorogens. *Accounts of Chemical Research*, *46*(11), 2441–2453.
Falco, C., Baccile, N., & Titirici, M.-M. (2011). Morphological and structural differences between glucose, cellulose and lignocellulosic biomass derived hydrothermal carbons. *Green Chemistry*, *13*(11), 3273–3281.
Feng, L., Zhu, C., Yuan, H., Liu, L., Lv, F., & Wang, S. (2013). Conjugated polymer nanoparticles: Preparation, properties. functionalization and biological applications. *Chemical Society Reviews*, *42*(16), 6620–6633.
Gao, X., Cui, Y., Levenson, R. M., Chung, L. W., & Nie, S. (2004). In vivo cancer targeting and imaging with semiconductor quantum dots. *Nature Biotechnology*, *22*(8), 969–976.
Hui, J., Zhang, X., Zhang, Z., Wang, S., Tao, L., Wei, Y., et al. (2012). Fluoridated HAp:Ln3+ (Ln = Eu or Tb) nanoparticles for cell-imaging. *Nanoscale*, *4*(22), 6967–6970.
Kim, H.-Y., Han, J.-A., Kweon, D.-K., Park, J.-D., & Lim, S.-T. (2013). Effect of ultrasonic treatments on nanoparticle preparation of acid-hydrolyzed waxy maize starch. *Carbohydrate Polymers*, *93*(2), 582–588.
Kim, J., Piao, Y., & Hyeon, T. (2009). Multifunctional nanostructured materials for multimodal imaging, and simultaneous imaging and therapy. *Chemical Society Reviews*, *38*(2), 372–390.
Kim, S., Ohulchanskyy, T. Y., Pudavar, H. E., Pandey, R. K., & Prasad, P. N. (2007). Organically modified silica nanoparticles co-encapsulating photosensitizing drug and aggregation-enhanced two-photon absorbing fluorescent dye aggregates for two-photon photodynamic therapy. *Journal of the American Chemical Society*, *129*(9), 2669–2675.
Lamanna, M., Morales, N. J., García, N. L., & Goyanes, S. (2013). Development and characterization of starch nanoparticles by gamma radiation: Potential application as starch matrix filler. *Carbohydrate Polymers*, *97*(1), 90–97.
Leung, C. W. T., Hong, Y., Chen, S., Zhao, E., Lam, J. W., & Tang, B. Z. (2013). A photostable AIE luminogen for specific mitochondrial imaging and tracking. *Journal of the American Chemical Society*, *135*(1), 62–65.
Li, J., Zhu, Y., Li, W., Zhang, X., Peng, Y., & Huang, Q. (2010). Nanodiamonds as intracellular transporters of chemotherapeutic drug. *Biomaterials*, *31*(32), 8410–8418.
Li, K., & Liu, B. (2014). Polymer-encapsulated organic nanoparticles for fluorescence and photoacoustic imaging. *Chemical Society Reviews*, http://dx.doi.org/10.1039/C1034CS00014E
Li, Y., Tan, Y., Ning, Z., Sun, S., Gao, Y., & Wang, P. (2011). Design and fabrication of fluorescein-labeled starch-based nanospheres. *Carbohydrate Polymers*, *86*(1), 291–295.
Liu, M., Zhang, X., Yang, B., Deng, F., Ji, J., Yang, Y., et al. (2014). Luminescence tunable fluorescent organic nanoparticles from polyethyleneimine and maltose: Facile preparation and bioimaging applications. *RSC Advances*, *4*(43), 22294–22298.
Liu, M., Zhang, X., Yang, B., Liu, L., Deng, F., Zhang, X., et al. (2014). Polylysine crosslinked AIE dye based fluorescent organic nanoparticles for biological imaging applications. *Macromolecular Bioscience*, http://dx.doi.org/10.1002/mabi.201400140
Liu, S., Zhang, H., Qiao, Y., & Su, X. (2012). One-pot synthesis of ternary $CuInS_2$ quantum dots with near-infrared fluorescence in aqueous solution. *RSC Advances*, *2*(3), 819–825.
Luo, P. G., Yang, F., Yang, S.-T., Sonkar, S. K., Yang, L., Broglie, J. J., et al. (2014). Carbon-based quantum dots for fluorescence imaging of cells and tissues. *RSC Advances*, *4*(21), 10791–10807.
Ma, X., Jian, R., Chang, P. R., & Yu, J. (2008). Fabrication and characterization of citric acid-modified starch nanoparticles/plasticized-starch composites. *Biomacromolecules*, *9*(11), 3314–3320.
Michalet, X., Pinaud, F., Bentolila, L., Tsay, J., Doose, S., Li, J., et al. (2005). Quantum dots for live cells, in vivo imaging, and diagnostics. *Science*, *307*(5709), 538–544.
Mitra, S., Chandra, S., Kundu, T., Banerjee, R., Pramanik, P., & Goswami, A. (2012). Rapid microwave synthesis of fluorescent hydrophobic carbon dots. *RSC Advances*, *2*(32), 12129–12131.
Moreira, F. K., Pedro, D. C., Glenn, G. M., Marconcini, J., & Mattoso, L. H. (2013). Brucite nanoplates reinforced starch bionanocomposites. *Carbohydrate Polymers*, *92*(2), 1743–1751.
Qi, H., Liu, M., Xu, L., Feng, L., Tao, l., Ji, Y., et al. (2013). Biocompatibility evaluation of aniline oligomers with different end-functional groups. *Toxicology Research*, *2*(6), 427–433.
Qin, A., Lam, J. W., & Tang, B. Z. (2012). Luminogenic polymers with aggregation-induced emission characteristics. *Progress in Polymer Science*, *37*(1), 182–209.
Qin, W., Ding, D., Liu, J., Yuan, W. Z., Hu, Y., Liu, B., et al. (2012). Biocompatible nanoparticles with aggregation-induced emission characteristics as

far-red/near-infrared fluorescent bioprobes for in vitro and in vivo imaging applications. *Advanced Functional Materials*, *22*(4), 771–779.
Rosi, N. L., & Mirkin, C. A. (2005). Nanostructures in biodiagnostics. *Chemical Reviews*, *105*(4), 1547–1562.
Sena, M., & Gao, X. (2010). Designing multifunctional quantum dots for bioimaging, detection, and drug delivery. *Chemical Society Reviews*, *39*(11), 4326–4354.
Shi, A.-m., Li, D., Wang, L.-j., Li, B.-z., & Adhikari, B. (2011). Preparation of starch-based nanoparticles through high-pressure homogenization and miniemulsion cross-linking: Influence of various process parameters on particle size and stability. *Carbohydrate Polymers*, *83*(4), 1604–1610.
Shi, A.-m., Wang, L.-j., Li, D., & Adhikari, B. (2013). Suspensions of vacuum-freeze dried starch nanoparticles: Influence of NaCl on their rheological properties. *Carbohydrate Polymers*, *94*(2), 782–790.
Tay, S. H., Pang, S. C., & Chin, S. F. (2012). Facile synthesis of starch-maleate monoesters from native sago starch. *Carbohydrate Polymers*, *88*(4), 1195–1200.
Thomas, S. W. I., Joly, G. D., & Swager, T. M. (2007). Chemical sensors based on amplifying fluorescent conjugated polymers. *Chemical Reviews*, *107*(4), 1339–1386.
Tian, H., Deng, C., Lin, H., Sun, J., Deng, M., Chen, X., et al. (2005). Biodegradable cationic PEG-PEI-PBLG hyperbranched block copolymer: Synthesis and micelle characterization. *Biomaterials*, *26*(20), 4209–4217.
Titirici, M.-M., Antonietti, M., & Baccile, N. (2008). Hydrothermal carbon from biomass: A comparison of the local structure from poly- to monosaccharides and pentoses/hexoses. *Green Chemistry*, *10*(11), 1204–1212.
Wang, K., Yuan, X., Guo, Z., Xu, J., & Chen, Y. (2014). Red emissive cross-linked chitosan and their nanoparticles for imaging the nucleoli of living cells. *Carbohydrate Polymers*, *102*, 699–707.
Wang, X., Liu, H., Li, J., Ding, K., Lv, Z., Yang, Y., et al. (2014). A fluorogenic probe with aggregation-induced emission characteristics for carboxylesterase assay through formation of supramolecular microfibers. *Chemistry an Asian Journal*, *9*(3), 784–789.
Wei, W., Wang, L.-Y., Yuan, L., Wei, Q., Yang, X.-D., Su, Z.-G., et al. (2007). Preparation and application of novel microspheres possessing autofluorescent properties. *Advanced Functional Materials*, *17*(16), 3153–3158.
Wei, W., Yuan, L., Hu, G., Wang, L.-Y., Wu, J., Hu, X., et al. (2008). Monodisperse chitosan microspheres with interesting structures for protein drug delivery. *Advanced Materials*, *20*(12), 2292–2296.
Weissleder, R. (2006). Molecular imaging in cancer. *Science*, *312*(5777), 1168–1171.
Xie, F., Pollet, E., Halley, P. J., & Averous, L. (2013). Starch-based nano-biocomposites. *Progress in Polymer Science*, *38*(10), 1590–1628.
Yang, B., Zhang, Y., Zhang, X., Tao, L., Li, S., & Wei, Y. (2012). Facilely prepared inexpensive and biocompatible self-healing hydrogel: A new injectable cell therapy carrier. *Polymer Chemistry*, *3*(12), 3235–3238.
Yu, C., Wu, Y., Zeng, F., Li, X., Shi, J., & Wu, S. (2013). Hyperbranched polyester-based fluorescent probe for histone deacetylase via aggregation-induced emission. *Biomacromolecules*, *14*(12), 4507–4514.
Zhang, X., Hui, J., Yang, B., Yang, Y., Fan, D., Liu, M., et al. (2013). PEGylation of fluoridated HAp: Ln3+ nanorods for cell imaging. *Polymer Chemistry*, *4*(15), 4120–4125.
Zhang, X., Qi, H., Wang, S., Feng, L., Ji, Y., Tao, L., et al. (2012). Cellular responses of aniline oligomers: A preliminary study. *Toxicology Research*, *1*(3), 201–205.
Zhang, X., Wang, S., Liu, M., Hui, J., Yang, B., Tao, L., et al. (2013). Surfactant-dispersed nanodiamond: Biocompatibility evaluation and drug delivery applications. *Toxicology Research*, *2*(5), 335–346.
Zhang, X., Wang, S., Liu, M., Yang, B., Feng, L., Ji, Y., et al. (2013). Size tunable fluorescent nano-graphite oxides: Preparation and cell imaging applications. *Physical Chemistry Chemical Physics*, *15*(43), 19013–19018.
Zhang, X., Wang, S., Xu, L., Ji, Y., Feng, L., Tao, L., et al. (2012). Biocompatible polydopamine fluoresecent organic nanoparticles: Facile preparation and cell imaging. *Nanoscale*, *4*(18), 5581–5584.
Zhang, X., Wang, S., Zhu, C., Liu, M., Ji, Y., Feng, L., et al. (2013). Carbon-dots derived from nanodiamond: Photoluminescence tunable nanoparticles for cell imaging. *Journal of Colloid and Interface Science*, *397*(9), 39–44.
Zhang, X., Zhang, X., tao, L., Chi, Z., Xu, J., & Wei, Y. (2014). Aggregation induced emission-based fluorescent nanoparticles: Fabrication methodology and biomedical application. *Journal of Materials Chemistry B*, *2*(28), 4398–4414.
Zhang, X., Zhang, X., Yang, B., Hui, J., Liu, M., Liu, W., et al. (2014). PEGylation and cell imaging applications of AIE based fluorescent organic nanoparticles via ring-opening reaction. *Polymer Chemistry*, *5*(3), 689–693.
Zhang, X., Zhang, X., Yang, B., Liu, L., Hui, J., Liu, M., et al. (2014). Aggregation-induced emission dyes based luminescent silica nanoparticles: Facile preparation, biocompatibility evaluation and cell imaging applications. *RSC Advances*, *4*(20), 10060–10066.
Zhang, X., Zhang, X., Yang, B., Liu, M., Liu, W., Chen, Y., et al. (2013). Facile fabrication and cell imaging applications of aggregation induced emission dye based fluorescent organic nanoparticles. *Polymer Chemistry*, *4*(16), 4317–4321.
Zhang, X., Zhang, X., Yang, B., Liu, M., Liu, W., Chen, Y., et al. (2014c). Fabrication of aggregation induced emission dye-based fluorescent organic nanoparticles via emulsion polymerization and their cell imaging applications. *Polymer Chemistry*, *5*(2), 399–404.
Zhang, X., Zhang, X., Yang, B., Liu, M., Liu, W., Chen, Y., et al. (2014d). Polymerizable aggregation induced emission dye based fluorescent nanoparticles for cell imaging applications. *Polymer Chemistry*, *5*(2), 356–360.
Zhang, X., Zhang, X., Yang, B., Liu, M., & Wei, Y. (2014). Facile fabrication of AIE based stable cross-linked fluorescent organic nanoparticles for cell imaging. *Colloids and Surface B Biointerfaces*, *116*(4), 739–744.
Zhang, X., Zhang, X., Yang, B., Zhang, Y., Liu, M., Liu, W., et al. (2014). Fabrication of water-dispersible and biocompatible red fluorescent organic nanoparticles via PEGylation of aggregate induced emission enhancement dye and their cell imaging applications. *Colloids and Surface B: Biointerfaces*, *1*(1), 435–441.
Zhang, X., Zhang, X., Yang, B., Zhang, Y., & Wei, Y. (2014). A new class of red fluorescent organic nanoparticles: Non-covalent fabrication and cell imaging applications. *ACS Applied Materials and Interfaces*, *6*(5), 3600–3606.
Zhao, Q., Li, L., Li, F., Yu, M., Liu, Z., Yi, T., et al. (2008). Aggregation-induced phosphorescent emission (AIPE) of iridium (III) complexes. *Chemical Communications*, (6), 685–687.
Zhao, Z., Chen, S., Shen, X., Mahtab, F., Yu, Y., Lu, P., et al. (2010). Aggregation-induced emission, self-assembly, and electroluminescence of 4,4′-bis (1,2,2-triphenylvinyl) biphenyl. *Chemical Communications*, *46*(5), 686–688.